Langmuir

Article

pubs.acs.org/Langmuir

Toward Multifunctional "Clickable" Diamond Nanoparticles

Manakamana Khanal,[†] Volodymyr Turcheniuk,[†,‡,§] Alexandre Barras,[†] Elodie Rosay,[§] Omprakash Bande,[§] Aloysius Siriwardena,[§] Vladimir Zaitsev,[‡,∥] Guo-Hui Pan,[⊥] Rabah Boukherroub,[†] and Sabine Szunerits*[,†]

[†]Institute of Electronics, Microelectronics and Nanotechnology (IEMN), UMR-CNRS 8520, Université Lille 1, Cité Scientifique, 59655 Villeneuve d'Ascq, France

[‡]Taras Shevchenko University, 60 Vladimirskaya str., Kiev, Ukraine

[§]Laboratoire de Glycochimie des Antimicrobiens et des Agroressources (LG2A) (FRE 3517-CNRS), Université de Picardie Jules Verne, 33 Rue St Leu, 80039 Amiens, France

[∥]Chemistry Department, Pontifical Catholic University of Rio de Janeiro, Rua Marques de Sao Vicente, 225-Gavea, Rio de Janeiro, 22451-900, Brazil

[⊥]State Key Laboratory of Luminescence and Applications, Changchun Institute of Optics, Fine Mechanics and Physics, Chinese Academy of Sciences, 3888 Dong Nanhu Road, Changchun 130033, China

ABSTRACT: Nanodiamonds (NDs) are among the most promising new carbon based materials for biomedical applications, and the simultaneous integration of various functions onto NDs is an urgent necessity. A multifunctional nanodiamond based formulation is proposed here. Our strategy relies on orthogonal surface modification using different dopamine anchors. NDs simultaneously functionalized with triethylene glycol (EG) and azide ($-N_3$) functions were fabricated through a stoichiometrically controlled integration of the dopamine ligands onto the surface of hydroxylated NDs. The presence of EG functionalities rendered NDs soluble in water and biological media, while the $-N_3$ group allowed postsynthetic modification of the NDs using "click" chemistry. As a proof of principle, alkynyl terminated di(amido amine) ligands were linked to these ND particles.

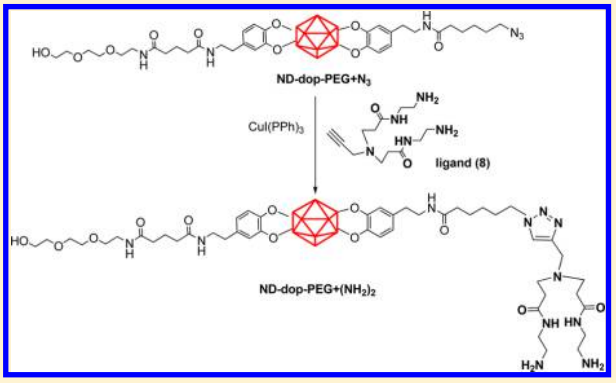

1. INTRODUCTION

Integrating biological components with nanomaterials for delivery of chemotherapeutic drugs or genetic material has been widely explored using a spectrum of approaches.[1−5] In many areas of biomedical research targeting molecules, drugs and imaging agents need to be simultaneously integrated on the nanostructure for the convenience of detection and targeted treatment. However, the implementation of multiple functionalities onto the surface of a nanoparticle is a difficult task and fraught with the possibility of nonselective cross reactions. Multifunctionalization strategies for gold[6] or magnetic particles have been recently reported.[7,8] Among the nanomaterials currently being considered are nanodiamonds (NDs).[9] One of the advantages of NDs over other carbon-based materials such as fullerenes and carbon nanotubes is that they are completely inert, optically transparent, and biocompatible and can be functionalized in many ways depending on their intended ultimate application.[10−16] Although *in vivo* toxicity of nanoparticles is dependent on specific surface characteristics, ND particles did not induce significant cytotoxicity in a variety of cell lines[17−20] and were used in various biomedical applications.[4,5,14,15,21−23]

While there have been diverse surface engineering strategies, currently, there are only three reports for the formation of orthogonally functionalized NDs.[24−27] Our group has shown lately that hydroxylated NDs (ND−OH) can be directly functionalized by dopamine derivatives.[10] Motivated by the ease by which functional groups like azide and others can be introduced via the dopamine terminal amine groups, we investigate in this work the possibility of using dopamine chemistry for the formation of multifunctional NDs. To validate the concept, a model material carrying triethylene glycol and azide modified dopamine anchors (dop−EG and dop−N_3) (Figure 1A) was fabricated. The functional azide moieties associated with the surface of the NDs could be furthermore chemoselectively conjugated to alkynyl terminated di(amido amine) ligands via a Cu(I) catalyzed cycloaddition reaction. The concept of "click" chemistry, introduced by K. B. Sharpless, is based on the copper(I) catalyzed triazole formation through the classic Huisgen 1,3-dipolar cycloaddition between azides and alkynes.[28,29] This cycloaddition reaction is irreversible and proceeds in quantitative yields and high selectivity. It is tolerant to a variety of solvents (including water) and can be performed in the presence of many other functional groups. "Click" chemistry related strategies have shown also to be very appealing for the

Received: February 18, 2015
Revised: March 17, 2015
Published: March 17, 2015

DOI: 10.1021/acs.langmuir.5b00643
Langmuir 2015, 31, 3926−3933

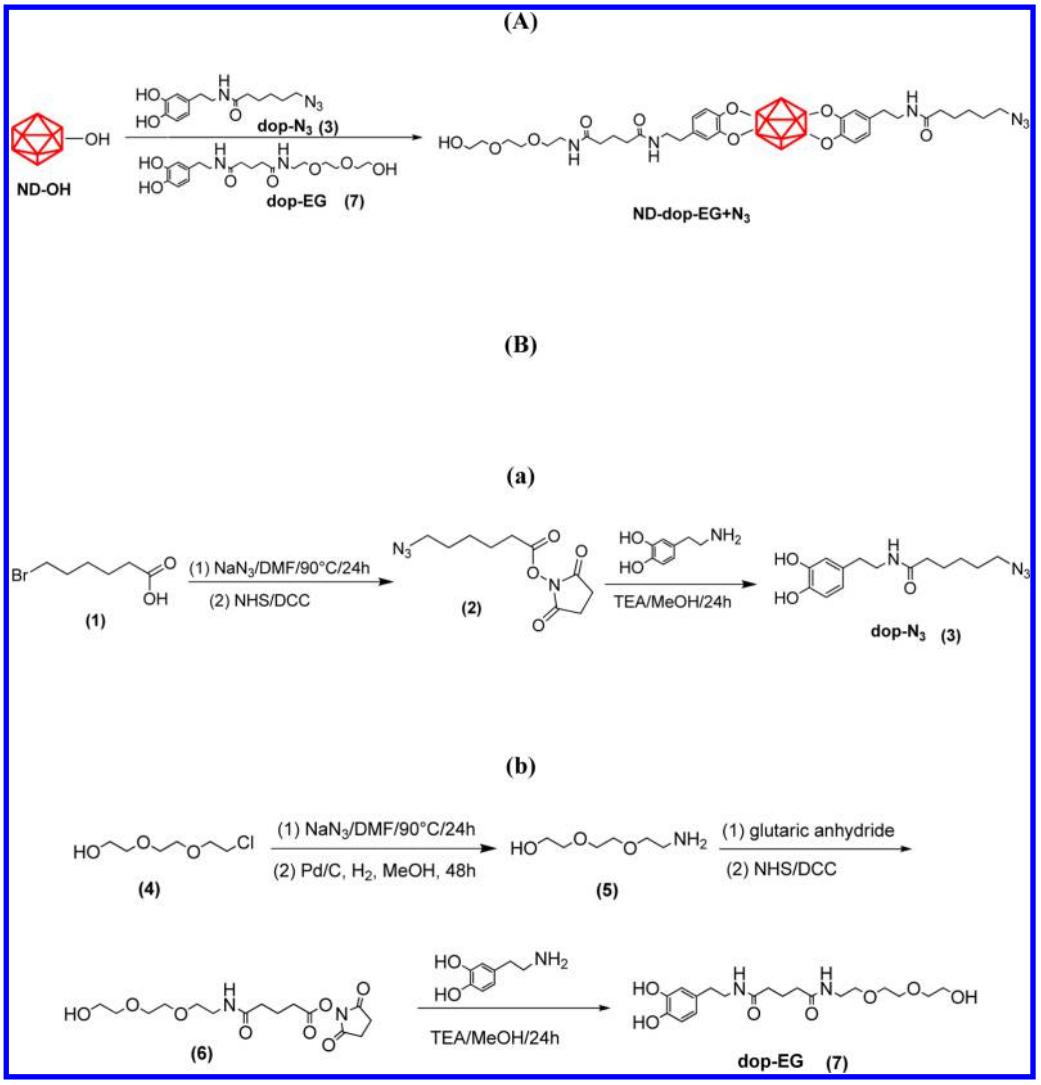

Figure 1. (A) Synthesis of multifunctional clickable NDs. (B) Synthetic routes to (a) azide-modified dopamine (dop−N_3) and (b) triethylene glycol-modified dopamine (dop−EG).

modification of NDs.[10,15,25−27,30−32] We have shown that, by "clicking" mannose ligands to NDs, the initial interaction of *Escherichia coli* (*E. coli*) with biotic as well as abiotic surfaces, a critical step in surface colonization and biofilm formation by this bacterium, can be inhibited.[15,32] The "clicking" of a boronic acid derivative to azide-terminated NDs gave ND particles which are able to reduce Hepatitis C viral infectivity through their effective blocking of viral entry.[21] NDs with "clicked" fluorescent tags and cyclic RGD peptide were recently reported by Cigler and co-workers to allow selective targeting of integrin $\alpha_v\beta_3$ receptors on glioblastoma cells with high internalization efficacy.[25] Krueger and co-workers attached a carbon monoxide delivery agent via "click" chemistry to NDs and studied the photoactivated CO release to biological systems.[31] Zhao et al. reported on the interest of multifunctional NDs where targeting RGD peptide and Pt-based drugs were clicked onto polyglycerol coated NDs for the selective killing of U87MG cells over HeLa ones.[26]

2. EXPERIMENTAL SECTION

2.1. Materials. Hydroxyl-terminated nanodiamond particles (ND−OH) and amine-terminated nanodiamonds (ND−NH_2) were purchased from International Technology Center (Raleigh, NC, USA) and display a primary average particle size of 4.0 nm. *N*,*N*′-Dicyclohexylcarbodiimide (DCC), *N*-hydroxysuccinimide (NHS), 4-dimethylaminopyridine (DMAP), copper(II) sulfate pentahydrate ($CuSO_4{\cdot}5H_2O$), L-ascorbic acid, 4-pentynoic acid, ethylenediaminetetraacetic acid (EDTA), triethylamine (TEA), acetonitrile, dichloromethane (DCM), methanol (MeOH), ethanol (EtOH), tetrahydrofuran (THF), hexane (Hex), ethyl acetate (EtOAc) and dimethylformatide (DMF) were obtained from Sigma-Aldrich and used without further purification.

CuI(PPh_3) was synthesized as described in the literature.[33] In short, a solution of triphenyl phosphine (0.69 g, 2.63 mmol) in 10 mL of acetonitrile was added to a solution of CuI (0.5 g, 2.63 mmol) in the same solvent (50 mL). A complex started to precipitate after a few seconds. The mixture was stirred for 1 h, and then, the precipitate was filtered, washed with acetonitrile, and vacuum-dried (yield 80%).

The alkynyl terminated di(amido amine) ligand was synthesized as described in the literature.[34]

2.2. Synthesis of Different Ligands. *2.2.1. Synthesis of 1-(6-{[2-(3,4-Dihydroxyphenyl)ethyl]amino}-6-oxohexyl)triaza-1,2-dien-2-ium (**3**). Synthesis of 6-Azidohexanoic N-Hydroxysuccinimide Ester (**2**).* A mixture of bromohexanoic acid (**1**) (4 g, 0.02 mmol) in DMF and sodium azide (NaN_3, 2.77 g, 0.04 mmol) was heated to 95 °C under stirring overnight. The solvent was evaporated under reduced pressure, and the product was diluted with water and extracted using DCM to give 6-azidohexanoic (**2**) as yellow oil. To the solution of 6-azidohexanoic acid (**2**) (1.95 g, 0.1 mmol) in dichloromethane was added dicyclohexycarbodiimide (2.56 g, 0,01 mmol) and *N*-hydroxysuccinimide

DOI: 10.1021/acs.langmuir.5b00643
Langmuir 2015, 31, 3926−3933

Table 1. Physico-Chemical Properties of Different NDs Used in This Work

sample	d (nm)	PI[a]	ζ (mV)	C 1s	O 1s	N 1s
ND−OH	79 ± 13	0.246 ± 0.002	22 ± 2	88.4	10.1	1.5
ND−dop−EG+N_3	120 ± 19	0.358 ± 0.012	25 ± 1	77.4	12.7	9.9
ND−dop−EG+$(NH_2)_2$	130 ± 19	0.357 ± 0.012	43 ± 1	70.8	12.9	16.3

[a]Polydispersity index; mean ± SD, n = 3.

(1.43 g, 0.01 mmol) and the mixture stirred overnight at room temperature. The solution was filtrated and the filtrate evaporated under reduced pressure to give 6-azidohexanoic *N*-hydroxysuccinimide ester (**2**) (2.8 g). ^{1}H NMR (300 MHz, $CDCl_3$) δ 3.35−3.27 (t, 2H), 2.82 (s, 4H, succinimide), 2.65−2.58 (t, 2H), 1.82−1.76 (m, 2H), 1.65−1.60 (m, 2H), 1.54−1.49 (m, 2H). MS (ESI): m/z (%) = 255 $[M + Na]^+$.

*Synthesis of 1-(6-{[2-(3,4-Dihydroxyphenyl)ethyl]amino}-6-oxohexyl)triaza-1,2-dien-2-ium (**3**).* Dopamine hydrochloride (162.5 mg, 0.86 mmol) was mixed with triethylamine (0.155 mL, 1.12 mmol) in methanol. 6-Azidohexanoic *N*-hydroxysuccinimide ester (**2**) (200 mg, 0.86 mmol) was added and then stirred overnight at room temperature under argon. The product was extracted using dichloromethane and washed with water. The organic layer was dried ($MgSO_4$) and evaporated under vacuum. Purification of compound **3** was done by flash column chromatography with EtOAc:Hex = 3:1 as eluent to give compound **3** (150 mg, 68%) as a slightly yellow oil. ^{1}H NMR (300 MHz, DMSO-d6) δ 8.66 (s, 2H), 7.79−7.76 (t, J = 10.9, 1H), 6.63−6.60 (d, J = 7.9, 1H), 6.55 (s, 1H), 6.43−6.39 (d, J = 10.1, 1H), 3.29−3.27 (d, J = 6.9, 2H), 3.19−3.12 (q, J = 20.5, 2H), 2.05−2.00 (t, J = 14.6, 2H), 1.56−1.43 (m, J = 36.2, 4H), 1.31−1.23 (d, J = 24.5, 2H). ^{13}C NMR (75 MHz, DMSO-d6) δ 165,56 (s), 144.35 (s), 143.25 (s), 135.54 (d), 120.34 (s), 117.33 (s), 114.55 (s), 49.79 (s), 40.57 (s), 35.38 (s), 34.41 (s), 29.53 (s), 25.45 (s), 24.92 (s). MS (ESI): m/z (%) = 319 $[M + Na]^+$.

*2.2.2. Synthesis of Ethylene Glycol Terminated Dopamine (dop−EG) (**7**). Synthesis of 2-[2-(2-Aminoethoxy)ethoxy]ethanol (**5**).* To a DMF solution of 2-[2-(2-chloroethoxy)ethoxy]ethanol (**4**) (4.79 g, 0.031 mmol), sodium azide (2 g, 0.046 mmol) was added and the reaction mixture was stirred at 90 °C for 24 h. The mixture was filtered, the solvent evaporated under reduced pressure, diluted with dichloromethane, washed with water, dried with $MgSO_4$, and evaporated to give 2-[2-(2-azidoethoxy)ethoxy]ethanol (4.6 g; 90%) as a yellow oil. ^{1}H NMR (300 MHz, $CDCl_3$) δ 3.75−3.68 (broad, 2H) 3.67−3.63 (m, 6H), 3.59−3.57 (m, 2H), 3.39−3.36 (t, 2H). MS (ESI): m/z (%) = 184 $[M + Na]^+$.

2-[2-(2-Azidoethoxy)ethoxy]ethanol (4 g, 0.025 mmol) and Pd/C (1.3 g) in methanol were stirred for 48 h at room temperature under hydrogen. The Pd/C was filtered off, and the solution was evaporated to give 2-[2-(2-aminoethoxy)ethoxy]ethanol (**5**) (3.2 g; 96%) as a yellow oil. ^{1}H NMR (300 MHz, $CDCl_3$) δ 3.77−3.73 (m, 3H), 3.70−3.67 (m, 5H), 3.65−3.61 (m, 3H), 3.58−3.54 (t, 2H). MS (ESI): m/z (%) = 157 $[M + Na]^+$.

*Synthesis of 5-[(2,5-Dioxopyrrolidin-1-yl)oxy]-N-{2-[2-(2-hydroxyethoxy)ethoxy]ethyl}-5-oxopentan Amide (**6**).* 2-[2-(2-Aminoethoxy)ethoxy]ethanol (**5**) (3.2 g, 0.02 mmol) and glutaric anhydride (2.7 g, 0.02 mmol) were mixed in THF overnight at room temperature. After solvent evaporation, 5-({2-[2-(2-hydroxyethoxy)-ethoxy]ethyl}amino)-5-oxopentanoic acid (5.2 g, 92%) was obtained as a yellow oil. ^{1}H NMR (300 MHz, $CDCl_3$) δ 7.35−7.02 (broad, J = 49.9 Hz, 1H), 6.81−6.69 (t, J = 34.4 Hz, 1H), 3.80−3.57 (d, J = 70.2 Hz, 9H), 3.48−3.43 (m, J = 15.0 Hz, 1H), 2.79−2.74 (t, J = 13.4 Hz, 2H), 2.47−2.38 (m, J = 26.4 Hz, 3H), 2.34−2.29 (t, J = 16.0 Hz, 1H), 2.08−1.96 (m, J = 35.6 Hz, 3H), 1.87−1.84 (t, J = 6.6 Hz, 1H). MS (ESI): m/z (%) = 262 $[M - H]^-$.

5-({2-[2-(2-Hydroxyethoxy)ethoxy]ethyl}amino)-5-oxopentanoic acid (4.6 g, 0.0174 mmol) and DCC (3.63 g, 0.0175 mmol) were dissolved in dichloromethane. NHS (2.02 g, 0.0175 mmol) in DCM was added, and the reaction mixture was stirred overnight at room temperature. After filtration and solvent evaporation, compound **6** (5.2 g; 83%) was obtained as a yellow oil. The crude product was used in the next step without further purification. ^{1}H NMR (300 MHz, MeOD) δ 4.4.29−4.21 (s, 1H), 3.76−3.36 (m, 8H), 2.88 (s, 4H), 2.79−2.7 (m, 2H), 2.58−2.52 (m, J = 19.8 Hz, 1H), 2.47−2.27 (m, 3H), 2.09−2.00 (m, 2H), 1.92−1.85 (m, 1H). ^{13}C NMR (75 MHz, MeOD) δ 170.50 (d), 168.60 (d), 70.17 (s), 68.77 (s), 63.35 (s), 39.00 (s), 34.09 (s), 32.72 (s), 29.49 (s), 25.16 (s, succinic C−C), 20.55 (s), 19.69 (s). MS (ESI): m/z (%) = 367 $[M + Na]^+$.

*Synthesis of N1-(3,4-Dihydroxyphenethyl)-N5-{2-[2-(2hydroxyethoxy)ethoxy]ethyl}pentane Diamide (**7**) (dop−EG).* To a solution of dopamine hydrochloride (104.7 mg, 0.76 mmol) and TEA (0.137 mL, 0.98 mmol) in MeOH was added compound **6** (200 mg, 0.76 mmol), and the mixture was stirred at room temperature for 24 h under argon. Purification by flash column chromatography using EtOAc:-MeOH:H_2O = 5:1:0.5 as an eluent gave compound **7** (160 mg; 69%) as a brown-yellow oil. ^{1}H NMR (300 MHz, MeOD) δ 6.70−6.67 (m, J = 4.8 Hz, 11.6, 2H), 6.56−6.53 (d, J = 8.1 Hz, 1H), 4.26−4.17 (m, J = 26.1 Hz, 1H), 3.75−3.51 (m, J = 70.8 Hz, 6H), 3.42−3.27 (m, J = 43.6 Hz, 6H), 2.69−2.59 (t, J = 30.3 Hz, 2H), 2.37−2.13 (m, J = 73.5 Hz, 6H), 1.94−1.84 (d, J = 28.7 Hz, 2H). ^{13}C NMR (75 MHz, MeOD) δ 173.60 (s), 145.95 (s), 144.13 (s), 130.66 (d), 119.69 (s), 115.53 (s), 114.99 (s), 70.12 (s), 69.83 (s), 69.17 (s), 68.76 (s), 63.17 (s), 40.76 (s), 38.92 (s), 34.50 (s), 32.69 (s), 24.88 (s), 21.84 (s), 21.02 (s). MS (ESI): m/z (%) = 421 $[M + Na]^+$.

2.3. Modification of Nanodiamonds. *2.3.1. Functionalization with Dopamine Ligands.* Hydroxylated nanodiamonds (ND−OH) (5 mg mL^{-1}) in dry acetonitrile were reacted with dop−N_3 (**3**), dop−EG (**7**), or a mixture of dop−N_3 (**3**)/dop−EG (**7**) (6 mM) in a 1/1 ratio with ultrasonication in an ice bath with a horn-type sonotrode (amplitude 70%) for 8 h and then left at room temperature for 12 h under stirring. The dopamine-functionalized ND particles (ND−dop−N_3, ND−dop−EG, and ND−dop−EG+N_3) were separated by centrifugation at 10.000 rpm, purified through four consecutive wash/centrifugation cycles at 10.000 rpm with acetonitrile and finally oven-dried at 50 °C overnight.

*2.3.2. Postfunctionalization of ND−dop−N_3 and ND−dop−EG +N_3 with Alkynyl-Terminated Di(amido amine) (**8**).* Azide-terminated NDs (ND−dop−N_3 and ND−dop−EG+N_3) were further modified with alkynyl terminated di(amido amine) (**8**) using "click" chemistry. The ND suspension (5 mg mL^{-1}) in dry DMF (8 mL) was sonicated for 30 min before alkynyl terminated di(amido amine) (**8**) (20 mg) and a catalytic amount of CuI(PPh_3) (10 mol %) were added and the mixture reacted for 48 h at 80 °C. The functionalized particles were separated by centrifugation at 10.000 rpm and purified through four consecutive washing/centrifugation cycles at 10.000 with DMF. Finally, the particles were washed with an aqueous solution of EDTA (1 mM, three times) to ensure that all the catalyst was removed and once with MQ water. The resulting NDs were oven-dried overnight at 50 °C.

2.4. Sample Characterization. *X-ray Photoelectron Spectroscopy (XPS).* X-ray photoelectron spectroscopy (XPS) measurements were performed with an ESCALAB 220 XL spectrometer from Vacuum Generators featuring a monochromatic Al Kα X-ray source (1486.6 eV) and a spherical energy analyzer operated in the CAE (constant analyzer energy) mode (CAE = 100 eV for survey spectra and CAE = 40 eV for high-resolution spectra), using the electromagnetic lens mode. No flood gun source was needed due to the conducting character of the substrates. The angle between the incident X-rays and the analyzer is 58°. The detection angle of the photoelectrons is 30°.

FTIR Spectroscopy. Fourier transformed infrared (FTIR) spectra in transmission mode were recorded using a ThermoScientific FTIR instrument (Nicolet 8700) with a resolution of 4 cm^{-1}. Dried ND powder (1 mg) was mixed with KBr powder (100 mg) in an agate mortar. The mixture was pressed into a pellet under 10 tons load for 2−4 min, and the spectrum was recorded immediately. Sixteen

DOI: 10.1021/acs.langmuir.5b00643
Langmuir 2015, 31, 3926−3933

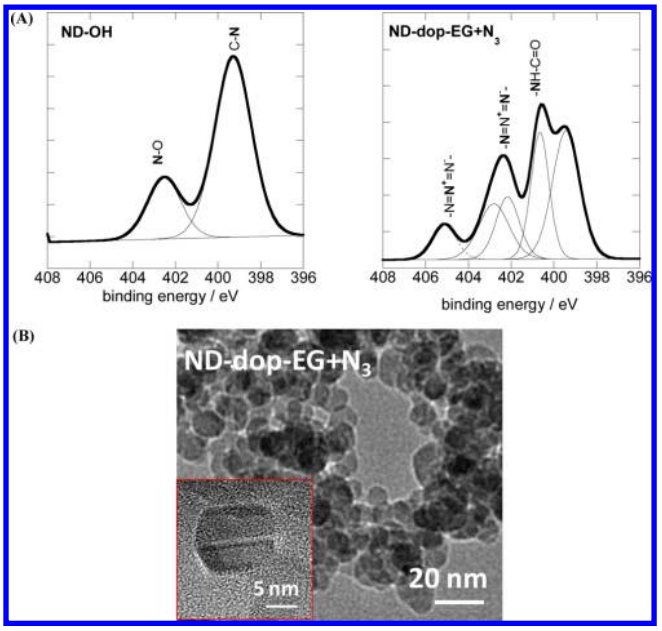

Figure 2. (A) N 1s high resolution XPS spectra of ND−OH and ND−dop−EG+N_3. (B) TEM images of ND−dop−EG+N_3.

accumulative scans were collected. The signal from a pure KBr pellet was subtracted as a background.

Transmission Electron Microscopy (TEM). TEM measurements were performed on an FEI Tecnai G2-F20 microscope.

Particle Size Distribution. ND suspensions (20 μg mL^{-1}) in water were sonicated for 1 h. The particle size of the ND suspensions was measured at 25 °C using a Zetasizer Nano ZS (Malvern Instruments S.A., Worcestershire, U.K.) in 173° scattering geometry, and the zeta potential was measured using the electrophoretic mode.

3. RESULTS AND DISCUSSION

As a preliminary step toward the fabrication of multifunctional, "clickable" diamond particles (Figure 1A), triethylene glycol (EG) and azide-terminated dopamine ligands (dop−EG and dop−N_3) were synthesized according to the synthetic route presented in Figure 1B. Polyethylene glycol, a class of hydrophilic polymers with excellent water solubility and biocompatibility, is widely used for the surface capping of nanostructures to impart water dispersibility.[35] The conjugation of dop−EG (**7**) onto the surface of ND particles is expected to improve their dispersion in aqueous media. At the same time, the integration of EG functions should reduce the uptake of the nanoparticles by the mononuclear phagocyte system, which is important for their biomedical use. Dop−EG (**7**) is obtained in a multiple step reaction from 2-[2-(2-chloroethoxy)ethoxy]ethanol (**4**). The formation of an amide bond between the terminal amine group of dopamine and the activated ester of 5-({2-[2-(2-hydroxyethoxy)ethoxy]ethyl}-amino)-5-oxopentanoic acid (**6**) resulted in dop−EG. Azide-terminated dopamine was synthesized in an analogous manner to dop−EG, through amide bond formation between dopamine and the activated ester for 6-azidohexanoic acid (**2**) (Figure 1B).

Before proceeding to the orthogonal surface functionalization of hydroxylated ND, deagglomeration of the as-received particles, produced via detonation synthesis, was achieved through a bead-assisted sonic disintegration process (BASD) as reported by Liang et al.[36] The resulting ND−OH particles showed a hydrodynamic diameter of 79 ± 13 nm (Table 1) and a zeta potential of $\zeta = 22 \pm 2$ mV. The origin of the positive charges is still a point of debate but widely observed for oxygen-functionalized NDs.[15,37] XPS analysis of the deagglomerated ND−OH particles indicates the presence of 1.5 atom % nitrogen (Table 1). The N 1s high resolution core level spectrum of ND−OH particles shows bands at 402.75 and 399.2 eV assigned to N−O and C−N bonds present (Figure 2A). This nitrogen content might be partly responsible for the positive surface charge of ND−OH particles.

The simultaneous linkage of dop—N_3 (**3**) and dop—EG (**7**) to the surface of ND—OH was achieved by mixing the particles with a stoichiometric amount of both dopamine ligands (dop—N_3:dop—EG = 1:1) and sonicating the mixtures in an ice bath

Table 2. Influence of the Stoichiometry by Using Different Feed Ratios of dop+N_3 (3) and dop−EG (7)

ratio dop+N_3 (**3**)/dop−EG (**7**)	d (nm)	PI[a]	ζ (mV)	C 1s	O 1s	N 1s
1/2	105 ± 15	0.346 ± 0.012	23 ± 2	65.7	21.5	12.8
1/1	120 ± 19	0.358 ± 0.015	25 ± 1	77.4	12.7	9.9
2/1	123 ± 19	0.297 ± 0.017	24 ± 1	68.0	16.5	15.5
3/1	121 ± 19	0.324 ± 0.014	26 ± 1	60.8	20.3	18.9

[a]Polydispersity index; mean ± SD, n = 3.

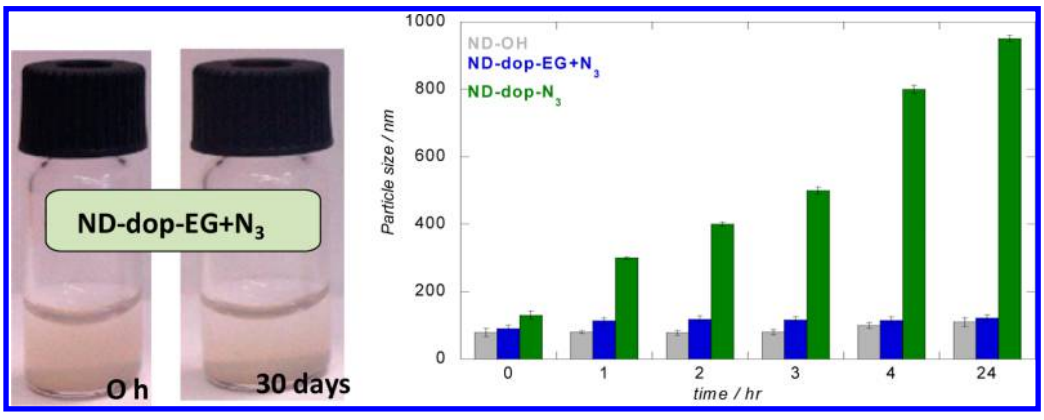

Figure 3. Photograph of suspensions of ND−dop−EG+N_3 (50 μg mL^{-1}) in PBS (pH 7.4, 0.1 M) at different time intervals together with a bar diagram of the change in particle size of ND−OH (gray), ND−dop−EG+N_3 (blue), and ND−dop−N_3 (green).

DOI: 10.1021/acs.langmuir.5b00643
Langmuir 2015, 31, 3926−3933

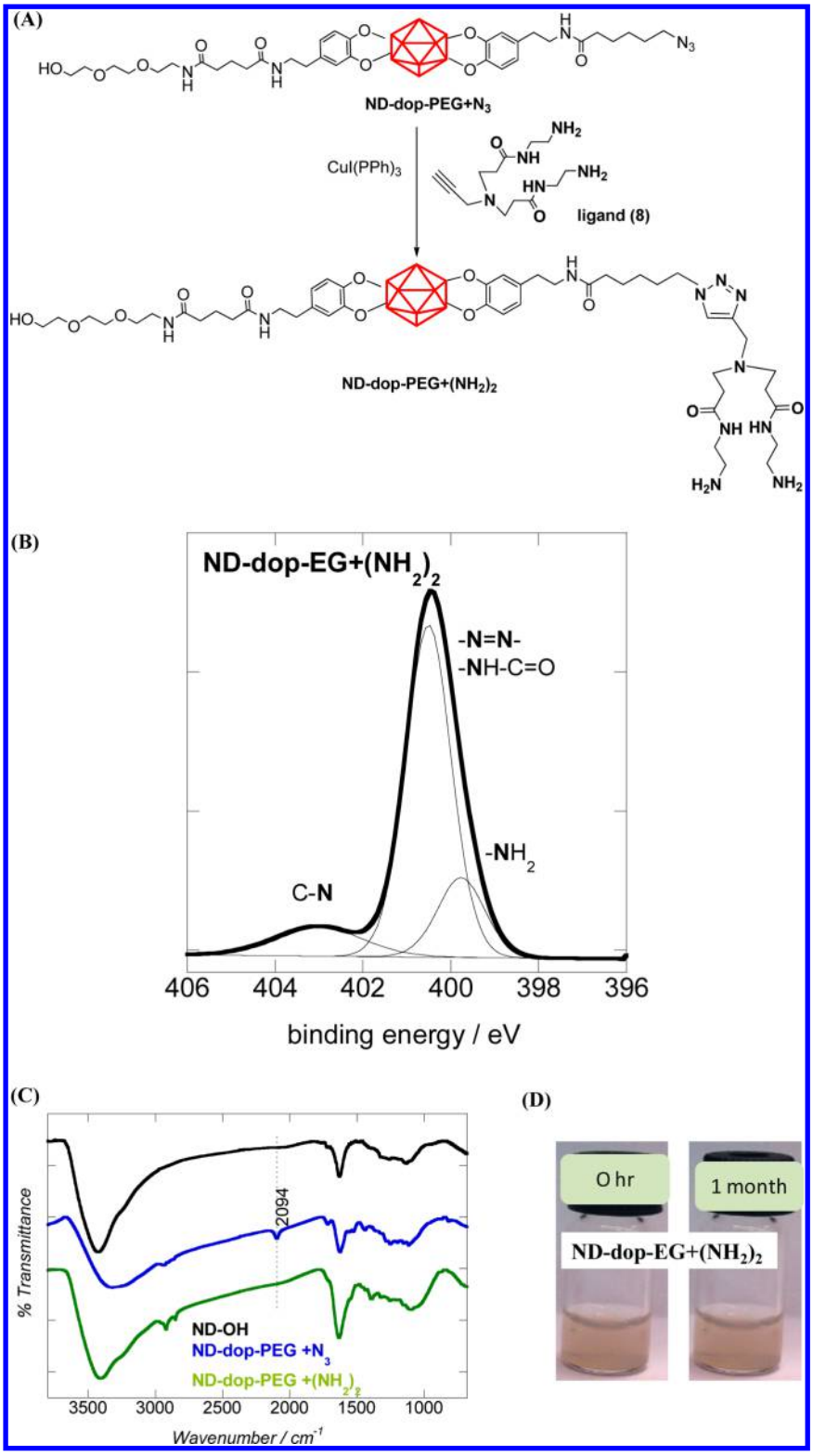

Figure 4. (A) Postfunctionalization of ND−dop−EG+N_3 with alkynyl-terminated di(amido amine) ligand (**8**) in a Cu(I) "catalyzed click" reaction. (B) N 1s high resolution XPS spectra of ND−dop−EG+(NH_2). (C) FTIR spectra of ND−OH (black), ND−dop−EG+N_3 (blue), and after "click" reaction with alkynyl-terminated di(amido amine) ligand (**8**) (green). (D) Stability of ND−dop−EG+$(NH_2)_2$ in PBS over time.

with a horn-type sonotrode for 8 h. The successful synthesis of ND—dop—EG+N_3 particles is confirmed by XPS analysis. The total atomic percentage of nitrogen increased from the initial 1.5 atom % (ND—OH) to 9.9 atom % for ND—dop—EG+N_3 (Table 1). Assuming that the nitrogen component is only from the nanodiamond itself, the integration of dopamine ligands counts for 8.4 atom % (six nitrogen atoms). The presence of the three —NH—C═O linkages and the —N_3 group is furthermore confirmed by XPS analysis of the N 1s region (Figure 2A). Next to bands at 402.7 and 399.2 eV due to N—O and C—N of ND—OH itself, the contribution of the —N_3 group at 405.2 (—N═$\underline{N}^+$═N^-) and 401.9 eV (—$\underline{N}$═N^+═$\underline{N}^-$)

DOI: 10.1021/acs.langmuir.5b00643
Langmuir 2015, 31, 3926−3933

and the presence of the —NH—C═O linkage at 400.6 eV can be distinguished. The peak ratio of the —NH—C═O band over the sum of the azide bands at 405.2 and 401.9 eV is 1.05 and correlates well with the theoretical ratio 1. This suggests that the transfer ratio of dop—EG (**7**)/dop—N_3 (**3**) ligands onto ND—OH is equivalent to the concentration of the ligand in solution.

To prove the stoichiometric controllability of the postsynthetic modification, particles with different feed ratios of dop−N_3 (**3**) and dop−EG (**7**) were prepared. Table 2 shows that different feed ratios do not have a significant impact on the size and zeta-potential of the resulting NDs. From XPS quantification of the nitrogen component and by accounting for the 1.5 atom % nitrogen content from diamond itself, it becomes clear that a stoichiometric dopamine transfer takes place for dop−N_3/dop−EG ratios of 1/2, 1/1, and 2/3 accounting for approximately 8N, 6N, and 10N, respectively. However, increasing the dop−N_3/dop−EG ratio to 3/1 results in the integration of somewhat more dop−PEG over dop−N_3 and the stoichiometry is sacrificed.

Transmission electron microscopy (TEM) measurements of ND−dop−EG+N_3 particles are shown in Figure 2B. They reveal the presence of spherical particles with a mean diameter of 12 ± 4 nm obtained from the analysis of several thousands of nanoparticles. The surface modified layer could not be observed due to its high transparency to the electron beam. However, the hydrodynamic diameter of ND−dop−EG+N_3 is determined as 120 ± 12 nm due to partial aggregation in solution (Table 1). However, it remained unchanged over days, indicating good colloidal stability in aqueous media.

The colloidal stability of the ND−dop−EG+N_3 particles in phosphate buffer (PBS) was assessed through particle size measurements and compared to that of ND−OH, and when modified entirely with dop−N_3 (ND−dop−N_3) (Figure 3).[10] Suspensions of ND−dop−EG+N_3 particles in PBS show excellent dispersibility and stability over time. In the case of azide particles without EG units present, the particle size increased from 150 nm to around 600 nm in the short time span of 3 h. This indicates the interest of multifunctinal ND−dop−EG+N_3 particles over ND−dop−N_3 ones as prepared previously.[10]

Postfunctionalization of Azide Functions in ND—dop—EG+N_3 Particles with Alkyne-Terminated Ligands. For different applications, ND—dop—EG+N_3 particles need to sustain further chemical modifications without affecting their colloidal stability. One class of reactions that is very attractive for an efficient grafting of ligands is the so-called "click" chemistry.[38] In a proof of principle, the azide functions were reacted using branched structures such as the alkynyl terminated di(amido amine) ligand (**8**) (Figure 4A).[34] The success of the integration of ligand **8** onto ND—dop—EG+N_3 particles was evidenced by the drastic increase in the atomic percentage of the N 1s (16.3 atom %) component when compared to ND—dop—EG+N_3 particles (9.9 atom %) (Table 1). For comparison, the amount of nitrogen in commercially available ND—NH_2 is only 2.3 atom %. The high resolution N 1s XPS spectra of the formed ND—dop—EG+$(NH_2)_2$ particles (Figure 4B) reveals the conversion of the surface azide groups into the corresponding triazole functions by the absence of the characteristic azide band at 405.2 eV. The spectrum can be deconvoluted into bands at 402.6 eV (—C—N—), 400.4 eV (—N═N— and NH—C═O, incorporating also the band of the N—O from diamond itself), and 399.5 due to protonated NH_2 groups respectively and the diamond contribution.

The successful integration of ligand **8** was in addition confirmed by FTIR analysis (Figure 4C). ND−OH particles show a broad peak at 3400 cm^{-1} assigned to the vibration of surface hydroxyl groups and/or adsorbed water molecules, and an additional sharper one at 1633 cm^{-1} due to the bending mode $\delta_{(OH)}$ of surface hydroxyl groups on the NDs. In addition, the band at 1107 cm^{-1} is indicative of the presence of C−O−C− functions of cyclic ethers. The FTIR spectrum of the ND−dop−EG+N_3 particles displays a band at 2125 cm^{-1} characteristic of the $\nu_{as(N3)}$ stretching mode. In addition, a broad band between 3000 and 3600 cm^{-1} assigned to the vibration of surface amino groups and/or adsorbed water molecules is seen. The peak at 1625 cm^{-1} is most likely due to a superposition of the NH scissoring mode and the OH deformation mode of adsorbed water. Similar vibration modes were reported for amine-terminated ND particles prepared from hydroxyl-terminated ND particles functionalized with 3-aminopropyltrimethoxysilane.[5] The CH_2 stretching bands of the organic linker molecules were observed at 2855 and 2924 cm^{-1}. The broad band at 1105 cm^{-1} is indicative for the C−O−C stretching bonds from the dop−EG ligand. Successful "clicking" of ligand (**8**) to ND−dop−EG+N_3 particles results in the consumption of azide functions and their replacement with surface triazole groups. As a consequence, the $\nu_{as(N3)}$ stretching mode at 2094 cm^{-1} is absent in the FT-IR spectrum of the clicked product. The size of ND−dop−EG+$(NH_2)_2$ particles was estimated as 130 ± 19 nm, with a strongly positive zeta potential of 43 ± 1 mV. This might indicate the presence of partly protonated $-NH_3^+$ groups. The stability of the cationic NDs in PBS over time was remarkable, and no aggregation occurred over a time period of 1 month (Figure 4D).

4. CONCLUSION

In summary, multifunctional, "clickable" diamond nanoparticles have been successfully designed. The model material was formed through the integration of triethylene glycol modified dopamine and azide-functionalized dopamine ligands. Data obtained from XPS analysis suggest that the transfer of dop−EG and dop−N_3 ligands onto the surface of ND−OH is equivalent to the concentration of the ligand in solution. The colloidal stability of the formed ND−dop−EG+N_3 was highly improved and comparable to ND−OH. Chemoselective conjugation of an alkynyl terminated di(amido amine) ligand onto the azide functions of ND−dop−EG+N_3 particles using Cu(I) catalyzed "click" chemistry could be successfully carried out. The postfunctionalization had no significant effect on the stability of the nanostructures over time. While an alkynyl terminated di(amido amine) ligand was used here, the described concept is generally applicable to any molecule carrying propargyl arms, such as glycans, fluorescent molecules, etc. The implementation of other desired functions depending on the sought after application is possible, following the outlined strategy, making the concept of wide interest.

AUTHOR INFORMATION

Corresponding Author

*Phone: +33 3 62 53 17 25. Fax: +33 3 62 53 17 01. E-mail: sabine.szunerits@iri.univ-lille1.fr.

Notes

The authors declare no competing financial interest.

DOI: 10.1021/acs.langmuir.5b00643
Langmuir 2015, 31, 3926−3933

■ ACKNOWLEDGMENTS

Financial support from the Centre National de la Recherche Scientifique (CNRS), the Université Lille 1, and the Institut Universitaire de France (IUF) is gratefully acknowledged. Support from the European Union through an FP7-PEOPLE-IRSES (No. 269009) is acknowledged as well as French Ministry of Foreign Affairs for a doctoral fellowship for M.K.

■ REFERENCES

(1) Neves, V.; Heister, E.; Costa, S.; Tilmaciu, C.; Flahaut, E.; Soula, B.; Coley, H. M.; McFadden, J.; Silva, S. R. P. Design of double-walled carbon nanotubes for biomedical applications. *Nanotechnology* **2012**, *23*, 365102−365110.

(2) Feng, L. Z.; Zhang, S.; Liu, Z. Graphene based gene transfection. *Nanoscale* **2011**, *3*, 1252−1257.

(3) Pantarotto, D.; Singh, R.; McCarthy, D.; Erhardt, M.; Briand, J.-P.; Prato, M.; Kostarelos, K.; Bianco, A. Functionalized Carbon Nanotubes for Plasmid DNA Gene Delivery. *Angew. Chem., Int. Ed.* **2004**, *43*, 5242−5246.

(4) Chen, M.; Zhang, X.-Q.; Man, H. B.; Lam, R.; Chow, E. K.; Ho, D. Nanodiamond Vectors Functionalized with Polyethylenimine for siRNA Delivery. *J. Phys. Chem. Lett.* **2010**, *1*, 3167−3171.

(5) Zhang, X.-Q.; Chen, M.; Lam, R.; Xu, X.; Osawa, E.; Ho, D. Polymer-Functionalized Nanodiamond Platforms as Vehicles for Gene Delivery. *ACS Nano* **2009**, *3* (9), 2609−2616.

(6) Conde, J.; Ambrosone, A.; Sanz, V.; Hernandez, Y.; Marchesano, V.; Tian, F.; Child, H.; Berry, C. C.; Ibarra, M. R.; Baptista, P. V.; Toriglione, C.; de la Fuente, J. M. Design of Multifunctional Gold Nanoparticles for In Vitro and In Vivo Gene Silencing. *ACS Nano* **2012**, *6*, 8316−8324.

(7) Das, M.; Bandyopadhyay, D.; Mishra, D.; Datir, S.; Dhak, P.; Jain, S.; Kumar Maiti, T.; Basak, A.; Pramanik, P. "Clickable", Trifunctional Magnetite Nanoparticles and Their Chemoselective Biofunctionalization. *Bioconjugate Chem.* **2011**, *22*, 1181−1193.

(8) Mazur, M.; Barras, A.; Kuncser, V.; Galatanu, A.; Zaitzev, V.; Turcheniuk, K. V.; Woisel, P.; Lyskawa, J.; Laure, W.; Siriwardena, A.; Boukherroub, R.; Szunerits, S. Iron oxide magnetic nanoparticles with versatile surface functions based on dopamine anchors. *Nanoscale* **2013**, *5*, 2692−2702.

(9) Mochalin, V. N.; Shenderova, O. A.; Ho, D.; Gogotsi, Y. The properties and applications of nanodiamonds. *Nat. Nanotechnol.* **2012**, *7*, 11−23.

(10) Barras, A.; Lyskawa, J.; Szunerits, S.; Woisel, P.; Boukherroub, R. Direct functionalization of nanodiamond particles using dopamine derivatives. *Langmuir* **2011**, *27*, 12451−12457.

(11) Barras, A.; Szunerits, S.; Marcon, L.; Monfilliette-Dupont, N.; Boukherroub, R. Functionalization of diamond nanoparticles using "click" chemistry. *Langmuir* **2010**, *26* (16), 13168−13172.

(12) Krüger, A. Hard and soft: biofunctinalized diamond. *Angew. Chem., Int. Ed.* **2006**, *45*, 6426−6427.

(13) Krüger, A. New Carbon Materials: Biological Applications of Functionalized Nanodiamond Materials. *Chem.—Eur. J.* **2008**, *14*, 1382−1390.

(14) Hartmann, M.; Betz, P.; Sun, Y.; N, G. S.; Lindhorst, T. K.; Krueger, A. Saccharide-Modified Nanodiamond Conjugates for the Efficient Detection and Removal of Pathogenic Bacteria. *Chem.—Eur. J.* **2012**, *18*, 6485−6492.

(15) Barras, A.; Martin, F. A.; Bande, O.; Baumann, J. S.; Ghigo, J.-M.; Boukherroub, R.; Beloin, C.; Siriwardena, A.; Szunerits, S. Glycan-functionalized diamond nanoparticles as potent E. coli anti-adhesives. *Nanoscale* **2013**, *5*, 2307−2316.

(16) Rehor, I.; Mackova, H.; Filippov, S. K.; Kucka, J.; Proks, V.; Slegerova, J.; Turner, S.; Van Tendeloo, G.; Ledvina, M.; Hruby, M.; Cigler, P. Fluorescent Nanodiamonds with Bioorthogonally Reactive Protein-Resistant Polymeric Coatings. *ChemPlusChem* **2014**, *79*, 21−24.

(17) Marcon, L.; Riquet, F.; Vicogne, D.; Szunerits, S.; Bodart, J.-F.; Boukherroub, R. Cellular and in vivo toxicity of functionalized nanodiamond in Xenopus embryos. *J. Mater. Chem.* **2010**, *20*, 8064−8069.

(18) Liu, K.-K.; Cheng, C.-L.; Chang, C. C.; Chao, J.-I. Biocompatible and detectable carboxylated nanodiamond on human cell. *Nanotechnology* **2007**, *18*, 325102−325112.

(19) Schrand, A. M.; Huang, H.; Carlson, C.; Schlager, J. J.; Osawa, E.; Hussain, S. M.; Dai, L. Are diamond nanoparticles cytotoxic? *J. Phys. Chem. B* **2007**, *111*, 2−7.

(20) Yu, S.-J.; Kang, M.-W.; Chang, H.-C.; Chen, K.-M.; Yu, Y.-C. Bright fluorescent nanodiamonds: no photobleaching and low cytotoxicity. *J. Am. Chem. Soc.* **2005**, *127*, 17604−17605.

(21) Khanal, M.; Vausselin, T.; Barras, A.; Bande, O.; Turcheniuk, K.; Benazza, M.; Zaitsev, V.; Teodurescu, C. M.; Boukherroub, R.; Siriwardena, A.; Dubuisson, J.; Szunerits, S. Phenylboronic-Acid-Modified Nanoparticles: Potential Antiviral Therapeutics. *ACS Appl. Mater. Interfaces* **2013**, *5*, 12488−12498.

(22) Wehling, J.; Dringer, R.; Zare, R. N.; Maas, M.; Rezwan, K. Bactericidal Activity of Partially Oxidized Nanodiamonds. *ACS Nano* **2014**, *8*, 6475−6483.

(23) Martin, R.; Alvaro, M.; Herance, J. R.; Garcia, H. Fenton- Treated Functionalized Diamond Nanoparticles as Gene Delivery System. *ACS Nano* **2010**, *4*, 65−74.

(24) Meinhardt, T.; Lang, D.; Dill, H.; Krueger, A. Pushing the Functionality of Diamond Nanoparticles to New Horizons: Orthogonally Functionalized Nanodiamond Using Click Chemistry. *Adv. Funct. Mater.* **2011**, *21*, 494−500.

(25) Slegerova, J.; Hajek, M.; Rehor, I.; Sedlak, F.; Stursa, J.; Hruby, M.; Cigler, P. Designing the nanobiointerface of fluorescent nanodiamonds: highly selective targeting of glioma cancer cells. *Nanoscale* **2015**, *7*, 415.

(26) Zhao, L.; Xu, Y.-H.; Qin, H.; Abe, S.; Akasaka, T.; Chano, T.; Watari, F.; Kimura, T.; Komatsu, N.; Chen, X. Platinum on Nanodiamond: A Promising Prodrug Conjugated with Stealth Polyglycerol, Targeting Peptide and Acid-Responsive Antitumor Drug. *Adv. Funct. Mater.* **2014**, *24*, 5348.

(27) Rehor, I.; Slegerova, J.; Kucka, J.; Proks, V.; Petrakova, V.; Adam, M.-P.; Treussart, F.; Turner, S.; Bals, S.; Sacha, P.; Ledvina, M.; Wen, A. M.; Steinmetz, N. F.; Cigler, P. Fluorescent Nanodiamonds Embedded in Biocompatible Translucent Shells. *Small* **2014**, *10*, 1106.

(28) Rostovtsev, V. V.; Green, L. G.; Fokin, V. V.; Sharpless, K. B. A Stepwise Huisgen Cycloaddition Process: Copper(I)-Catalyzed Regioselective "Ligation" of Azides and Terminal Alkynes. *Angew. Chem., Int. Ed.* **2002**, *41*, 2596−2599.

(29) Kolb, H. C.; Finn, M. G.; Sharpless, K. B. Click Chemistry: Diverse Chemical Function from a Few Good Reactions. *Angew. Chem., Int. Ed.* **2001**, *40*, 2004−2021.

(30) Romanova, E. E.; Akiel, R.; Cho, F. H.; Takahashi, S. Grafting nitroxide radicals on nanodiamond surface using click chemistry. *J. Phys. Chem. A* **2013**, *117*, 11933.

(31) Dördelmann, G.; Meinhardt, T.; Sowik, T.; Krueger, A.; Schatzschneider, U. CuAAC click functionalization of azide-modified nanodiamond with a photoactivatable CO-releasing molecule (Photo-CORM) based on [Mn(CO)3(tpm)]. *Chem. Commun.* **2012**, *48*, 11528−11530.

(32) Khanal, M.; Larsonneur, F.; Raks, V.; Barras, A.; Baumann, J.-S.; Ariel Martin, F.; Boukherroub, R.; Ghigo, J.-M.; Ortiz Mettet, C.; Zaitsev, V.; Garcia Fernances, J. M.; Beloin, C.; Siriwardena, A.; Szunerits, S. Inhibition of type 1 fimbriae-mediated Escherichia coli adhesion and biofilm formation by trimeric cluster thiomannosides conjugated to diamond nanoparticles. *Nanoscale* **2015**, *7*, 2325−2335.

(33) Wang, Y.; Xiao, Y.; Thatt Yang Tan, T.; Ng, S.-C. Click chemistry for facile immobilization of cyclodextrin derivatives onto silica as chiral stationary phases. *Tetrahedron Lett.* **2008**, *49*, 5190−5191.

(34) Chen, L.; Chen, T.; Fang, W.; Wen, Y.; Lin, S.; Lin, J.; Cai, C. Synthesis and pH-responsive "schizophrenic" aggregation of a linear-dendron-like polyampholyte based on oppositely charged polypeptides. *Biomacromolecules* **2013**, *14*, 4320−4330.

(35) Hong, R.; Fischer, N. O.; Emrick, T.; Rotello, V. M. Surface PEGylation and Ligand Exchange Chemistry of FePt Nanoparticles for Biological Applications. *Chem. Mater.* **2005**, 4617−4621.

DOI: 10.1021/acs.langmuir.5b00643
Langmuir 2015, 31, 3926−3933

(36) Liang, Y.; Ozawa, M.; Krueger, A. A general procedure to functionalize agglomerating nanoparticles demonstrated on nanodiamond. *ACS Nano* **2009**, *3* (8), 2288−2296.
(37) Williams, O. A.; Hees, J.; Dieker, C.; Jager, W.; Kirste, L.; Nebel, C. E. Size-dependent reactivity of diamond nanoparticles. *ACS Nano* **2010**, *4*, 4824−4830.
(38) Moses, J. E.; Moorhouse, A. D. The growing applications of click chemistry. *Chem. Soc. Rev.* **2007**, *36*, 1249−1262.

DOI: 10.1021/acs.langmuir.5b00643
Langmuir 2015, 31, 3926−3933